ACS APPLIED MATERIALS & INTERFACES

Research Article

Cite This: ACS Appl. Mater. Interfaces 2018, 10, 20368−20376

www.acsami.org

# Computational Investigations of the Interaction between the Cell Membrane and Nanoparticles Coated with a Pulmonary Surfactant

Xuan Bai,[†,§] Ming Xu,[‡,§] Sijin Liu,[*,‡,§] and Guoqing Hu[*,†,§]

[†]State Key Laboratory of Nonlinear Mechanics (LNM), Institute of Mechanics, Chinese Academy of Sciences, Beijing 100190, China

[‡]State Key Laboratory of Environmental Chemistry and Ecotoxicology, Research Center for Eco-Environmental Sciences, Chinese Academy of Sciences, Beijing 100085, China

[§]University of Chinese Academy of Sciences, Beijing 100049, China

Supporting Information

**ABSTRACT:** When inhaled nanoparticles (NPs) come into the deep lung, they develop a biomolecular corona by interacting with the pulmonary surfactant. The adsorption of the phospholipids and proteins gives a new biological identity to the NPs, which may alter their subsequent interactions with cells and other biological entities. Investigations of the interaction between the cell membrane and NPs coated with such a biomolecular corona are important in understanding the role of the biofluids on cellular uptake and estimating the dosing capacity and the nanotoxicology of NPs. In this paper, using dissipative particle dynamics, we investigate how the physicochemical properties of the coating pulmonary surfactant lipids and proteins affect the membrane response for inhaled NPs. We pinpoint several key factors in the endocytosis of lipid NPs, including the deformation of the coating lipids, coating lipid density, and ligand−receptor binding strength. Further studies reveal that the deformation of the coating lipids consumes energy but on the other hand promotes the coating ligands to bind with receptors more tightly. The coating lipid density controls the amount of the ligands as well as the hydrophobicity of the lipid NPs, thus affecting the endocytosis kinetics through the specific and nonspecific interactions. It is also found that the hydrophobic surfactant proteins associated with lipids can accelerate the endocytosis process of the NPs, but the endocytosis efficiency mainly depends on the density of the coating surfactant lipids. These findings can help understand how the pulmonary surfactant alters the biocompatibility of the inhaled NPs and provide some guidelines in designing an NP complex for efficient pulmonary drug delivery.

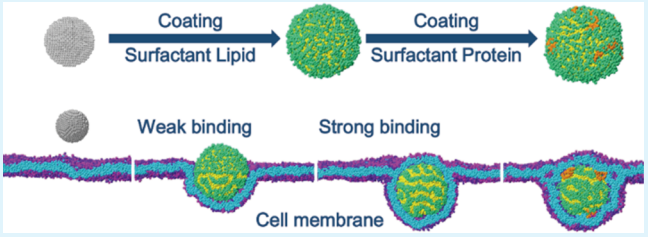


**KEYWORDS:** *endocytosis, pulmonary surfactant, nanoparticle, corona, dissipative particle dynamics simulation*

## 1. INTRODUCTION

Rapid development of the nanotechnology not only widens the applications of nanoparticles (NPs) in biological engineering[1,2] but also increases concerns in the risk of NPs.[3,4] The cellular internalization of the NPs is one of the crucial processes to estimate the dosing capacity and the nanotoxicology of NPs.[5−7] Depending on the types of cells and NPs, the NPs can enter cells via different pathways through specific and nonspecific interactions, such as phagocytosis, receptor-mediated endocytosis (RME), and direct penetration.[8,9] The RME is considered as one of the most efficient pathways for the NPs with a diameter of 25−50 nm.[9−11] In the RME process, the NPs are always coated with biopolymers or macromolecules or bioconjugated with functional groups that act as ligands to be recognized and bound by the receptors on the cell membrane. Current studies have shown that both the chemical and physical properties of the NPs, such as surface modification, shape, and stiffness, impact the RME process and cellular uptake further.[12−16]

Before NPs interact with cells, they always inevitably come in contact with the biological fluids (plasma, intestinal fluid, and pulmonary surfactant) first. Biomolecules in the biofluids selectively adsorb onto these NPs, forming the so-called biomolecular coronas that can change the surface properties and the biorecognition of the NPs and thus possibly alter the subsequent cellular uptake of the NPs.[5,17−19] Related works have shown that NPs via intravascular administration usually bind with serum protein coronas that decrease or increase the cellular uptake depending on the types of the pristine surface properties and the adsorbed proteins.[20−23] Lung, one of the organs directly contacting with the external environment, is another major route to take NPs, such as nanosized air pollutions and noninvasive drug delivery.[4,24,25] After being inhaled, the NPs will encounter the pulmonary surfactant when deposited in the deep lung and adsorb surfactant lipids and proteins based on their surface properties.[26−28] Several experiments have demonstrated that coating of the pulmonary surfactant can enhance the uptake of NPs by different lung cell

Received: April 25, 2018
Accepted: May 29, 2018
Published: May 29, 2018

Downloaded via UNIV OF SUSSEX on August 17, 2018 at 09:33:07 (UTC).
See https://pubs.acs.org/sharingguidelines for options on how to legitimately share published articles.


© 2018 American Chemical Society

DOI: 10.1021/acsami.8b06764
ACS Appl. Mater. Interfaces 2018, 10, 20368−20376

lines.[29−31] Although some experiments have been designed to investigate the pathways of the NPs incubated in a surfactant lipid matrix or bronchoalveolar lavage fluid, the associated mechanism at the molecular scale is hardly to identify because of the limitation of the available experimental techniques.[29,32] Mesoscale computer simulation, which has been widely applied in an NP−membrane interaction, can provide useful information related to the mechanics of the endocytosis from a molecular view.[33−38] Existent computational studies have shown that the physiochemical properties of the coating molecules (single-chain ligand,[39] hydrophilic polyethylene glycol polymer,[40] and human serum protein[41]) on NPs can impact the endocytosis process. However, to date, relevant studies on how coating of pulmonary surfactant lipids and proteins affects the interactions between NPs and the cell membrane are still scarce. Here, we introduce a dissipative particle dynamics (DPD) simulation method to investigate these interactions.[42]

Corona can be divided into two layers: one is called "hard corona", which tightly binds to the NP surface and lives long in an equilibrium state, and another is called "soft corona", which is loosely bound and can be rapidly exchanged with the biofluidic environment.[19] Considering that the hard corona is thought to be most determinant in physiological response,[5,18] we adopt the hard corona in the present simulations to focus on its effects on cellular uptake. Given that the coating lipids dominate the component of the lipoprotein corona, most of our simulations study the effect of the coating lipids on the cellular uptake using a core (hydrophobic NP)−shell (lipid monolayer) model, which is mapped from previous experimental and computational observation.[28,43,44] For clarity, the NPs coated only with surfactant lipids are called lipid NPs in the present simulations. Meanwhile, hydrophobic surfactant proteins (SPs) are always phospholipid-associated acting as a bridge between lipid layers[45,46] and can appear on the lipoprotein corona without disturbing the structure of the surfactant lipids.[28] Thus, we use the lipid NPs coated with extra hydrophobic SPs, that is, the lipoprotein NPs, to study the effect of the hydrophobic SP on endocytosis.

In this paper, we performed a comprehensive computational study on the effect of the physicochemical properties of the pulmonary surfactant on the endocytosis kinetics. First, we showed the wrapping pathway for the lipid NP by comparing with the pristine hydrophilic and hydrophobic NPs without coating ligands. Second, we described how the deformation of the coating lipids affected the endocytosis for the lipid NP. Then, we discussed how the coating lipid density influenced the cellular uptake at a different ligand−receptor bending strength. Finally, we studied the effect of the hydrophobic SPs on the wrapping kinetics by comparing the wrapping pathway of lipid NPs and lipoprotein NPs.

## 2. COMPUTATIONAL MODEL AND METHODOLOGY

**2.1. DPD Formulation.** The DPD technique, a mesoscopic coarse-grained (CG) method, was used in this work, which has been successfully and widely used in biomembrane simulation.[34,37,47] In the CG molecular dynamics, a cluster of atoms can be represented by one single bead to increase the temporal and spatial scale and each bead is governed by the Newton equation of motion

$$\frac{\mathrm{d}v_i}{\mathrm{d}t} = \frac{F_i}{m} \tag{1}$$

where the mass $m$ of a single bead is set to 1. The interaction between beads $i$ and $j$ consists of three types of forces: conservative force $F_{ij}^{\mathrm{C}}$, dissipative force $F_{ij}^{\mathrm{D}}$, and random force $F_{ij}^{\mathrm{R}}$. The total force on the bead $i$ can be expressed as

$$F_i = \sum_{i \neq j} F_{ij}^{\mathrm{C}} + F_{ij}^{\mathrm{D}} + F_{ij}^{\mathrm{R}} \tag{2}$$

where the sum runs over all beads $j$ within a certain cutoff radius $r_c$. The conservative force is a soft-repulsive force given by

$$F_{ij}^{\mathrm{C}} = a_{ij}(1 - \mathbf{r}_{ij})\hat{\mathbf{r}}_{ij} \tag{3}$$

where $a_{ij}$ represents the maximum repulsion between the beads $i$ and $j$, $\mathbf{r}_{ij} = (\mathbf{r}_i - \mathbf{r}_j)/r_c$, $r_{ij} = |\mathbf{r}_{ij}|$, and $\hat{\mathbf{r}}_{ij} = \mathbf{r}_{ij}/|r_{ij}|$. The dissipative force is taken as

$$F_{ij}^{\mathrm{D}} = -\gamma\omega_{\mathrm{D}}(\mathbf{r}_{ij})(\hat{\mathbf{r}}_{ij}\cdot\mathbf{v}_{ij})\hat{\mathbf{r}}_{ij} \tag{4}$$

where $\gamma$ represents the strength of friction, $\omega_{\mathrm{D}}(r_{ij}) = (1 - r_{ij})^2$, and $\mathbf{v}_{ij} = \mathbf{v}_i - \mathbf{v}_j$. The random force is given by

$$F_{ij}^{\mathrm{R}} = \sigma\omega_{\mathrm{R}}(\mathbf{r}_{ij})\xi_{ij}\hat{\mathbf{r}}_{ij} \tag{5}$$

where $\xi_{ij}$ is a zero-mean Gaussian random variable of unit variance, $\omega_{\mathrm{R}}(r_{ij}) = 1 - r_{ij}$, and $\sigma$ is a noise amplitude and equals to $\sqrt{2k_{\mathrm{B}}T\gamma}$. We also take $r_c$ as the characteristic length scale and $k_{\mathrm{B}}T$ as the characteristic energy scale. The characteristic time scale is defined as $\tau = \sqrt{mr_c^2/k_{\mathrm{B}}T}$. Equation 1 is integrated in time with a velocity-Verlet algorithm at $\sigma = 3$ and $\Delta t = 0.01\tau$. The simulation box is a $100r_c \times 100r_c \times 70r_c$ domain with periodic boundaries in $x$, $y$, and $z$ direction, where the particle density is 3. All simulations are performed in the NVT ensembles using LAMMPS package.[48]

**2.2. Simulation Model.** Figure 1 illustrates the CG DPD model of different components in our simulation. The NP with a diameter of $16r_c$ is formed by particle beads arranged on a face-centered cubic lattice to prevent other beads' insertion and constrained to move as a rigid body. The lipid molecule is

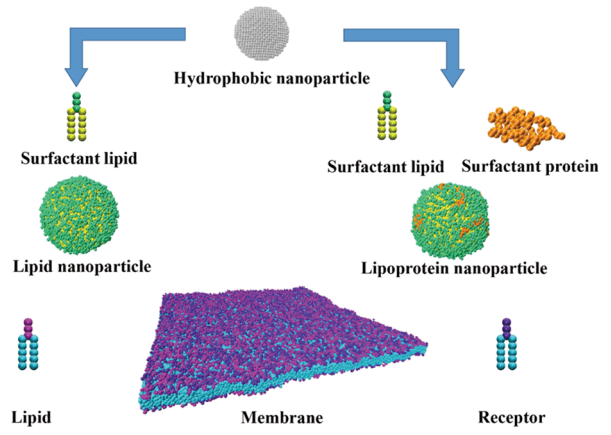


**Figure 1.** Schematic illustration of the models in computer simulations. Silver beads represent a NP, green beads represent surfactant lipid heads, yellow beads represent surfactant lipid tails, and orange beads represent hydrophobic proteins. The conformation of the lipid NP and lipoprotein NP is shown after equilibrated in pure water. The membrane is consisted of 5524 lipids and 5524 receptors. Magenta beads represent membrane lipid heads, cyan beads represent membrane lipid tails, and violet beads represent receptors.


DOI: 10.1021/acsami.8b06764
ACS Appl. Mater. Interfaces 2018, 10, 20368−20376

represented by the $H_3T_5$ CG model proposed by Groot and Rabone.[47] Here, the head groups are CG to three hydrophilic beads and every three carbon atoms of each alkyl chain are taken together as one hydrophobic bead, which is suitable for modeling the dipalmitoylphosphatidylcholine (DPPC) or dimyristoylphosphatidylcholine molecule. These lipids can assemble to a stable bilayer structure when immersed in water. Note that the water beads are not shown here for clarity. Considering that DPPC is the major component of the surfactant lipids, we also adopt this lipid model to represent the coating surfactant lipids on the NP. For modeling the hydrophobic SP, we map the CG models provided by the Martini force field to the DPD simulation. More details of the CG modeling method are given in the Supporting Information. Given that the surfactant lipids can provide biorecognition for NPs especially related to the clearance by pulmonary macrophages,[19,49] the surfactant lipid heads are considered as the ligands.[50] They can react with receptors, such as cell-penetrating peptides, in the membrane.[51] Meanwhile, 50% lipid heads of the membrane are considered as receptors, where the high ratio of receptors has been proved an efficient way to simulate the RME.[34,40,41] The ligand−receptor interaction parameter $a_{RL}$ is set to $0-15k_BT/r_c$ in the DPD parameter. In addition, to examine the interaction between the NP and the membrane at a higher ligand−receptor binding strength, we here introduce a soft Lennard-Jones (LJ) potential, which is defined by

$$U_{ij}^{\text{ligand-receptor}} = 4\varepsilon[(\sigma/\mathbf{r}_{ij})^{12} - (\sigma/\mathbf{r}_{ij})^{6}] + 0.22\varepsilon \quad (6)$$

where $\mathbf{r}_{ij} \leq r_c$, $\sigma = 0.624r_c$, and $\varepsilon$ represents the strength of the ligand−receptor reaction and ranges from $3k_BT$ to $5k_BT$.[34] Additionally, the repulsive force is set to be $25k_BT/r_c$ when it is larger than $25k_BT/r_c$ to guarantee the proper running of the DPD simulation. Given that the hydrophilic beads of the SP are highly polar and can strongly attract with the lipid heads, we also use this potential ($\varepsilon = 3k_BT$) to simplify such a strong interaction. Other interactions between beads $i$ and $j$ are followed by DPD formulation, and the exhaustive description of the adopted parameters is shown in the Supporting Information. One of the input scripts for the LAMMPS package and the script to create the bond list (format for the data file in the LAMMPS package) for the DPD protein model based on the Martini force field have been provided in the Supporting Information.

The lipid NPs and lipoprotein NPs are fully equilibrated in pure water for dozens of nanoseconds to obtain the initial conformation of the coating NPs, as shown in Figure 1. Then the equilibrated coating NPs are placed above the membrane in another simulation box to study the NP−membrane interaction. During the simulations of the NP−membrane interaction, to maintain the membrane at zero tension, the lipid number per area at the boundary is adjusted to equal to 1.1 by stretching or compressing the box.[37,40,41] By examining the membrane thickness and the lipid diffusion coefficient, we can convert the reduced DPD units to SI units.[52] The simulated value of the bilayer thickness is about $5r_c$ and the characteristic time scale can be obtained by the simulated lateral diffusion constants of the lipid bilayer.[53,54] In practice, the thickness of the DPPC bilayer is 4 nm and the in-plane diffusion coefficient is 5 $\mu m^2/s$ in the experiment.[52] We can yield $r_c = 0.8$ nm and $\tau = 24$ ps.

## 3. RESULTS AND DISCUSSION

**3.1. Different Pathways for Bare NPs and the Lipid NP.** First, 800 pulmonary surfactant lipids are coated onto an NP, resulting in an area per lipid of $1.00r_c^2$ at the core NP surface and $1.73r_c^2$ at the lipid NP surface. Unlike pristine NPs without ligands, the lipid NP can be internalized by the cell membrane via a unique wrapping pathway, as shown in Figure 2a. Generally, pristine NPs without ligands can hardly adhere to the cell membrane but can penetrate the membrane by an external force or using the dynamic bond.[34,55] Under some circumstances, hydrophobic NPs will enter into the lipid bilayer because of their preference to lipid hydrophobic tails in the water environment.[56] The lipid NP, like other NPs coated with biomolecules, can be engulfed by the cell membrane through an RME in similar wrapping ways.[39,40,57] Note that the lipid NPs wrapped by a lipid bilayer can be internalized through an external force generated by actin filaments.[58] Recent experiments have found that the silica NPs coated with surfactant lipids can only be detected in endosomes and lysosomes after cellular uptake, whereas the bare silica NPs were freely dispersed in the cytosol.[59] This indicated that the internalization of NPs underwent a membrane-wrapping process for lipid NPs but suffered the direct penetration of the bare NPs that will severely destroy the cell membrane, in accordance with our simulations. Next, we analyze the key factors in the endocytosis kinetics of the lipid NP.

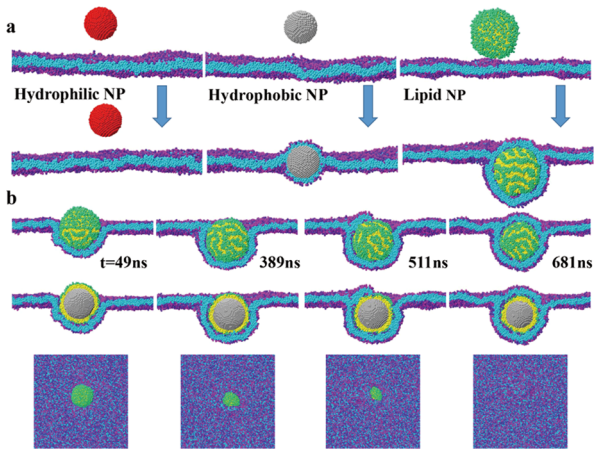


**Figure 2.** Representation of the pathway for lipid NPs. (a) Different pathways for bare NPs without ligands and lipid NPs. All of these simulations are taken for several million steps. (b) Representative DPD simulation snapshots for the endocytosis of lipid NPs (coated with 800 lipids) at a low ligand−receptor binding strength ($a_{RL} = 10$) in three different views.

A detailed time sequence of snapshots for the endocytosis of the lipid NP is displayed in Figure 2b. The whole endocytosis process can be divided into two parts: membrane bending stage ($t < 400$ ns) and monolayer protruding stage ($t > 400$ ns). During the simulation, the coating lipids at the contact region have a different morphology compared with those at the noncontact region. This is because the strong attractions between receptors and surfactant lipids cause their aggregations and lead to the conformational changes in the head groups of surfactant lipids. Surfactant lipid tails tend to contact with the tails of membrane lipids to make a splayed lipid conformation, which is considered as a typical model for initial membrane fusion.[60] Previous studies have pointed that the conformational


DOI: 10.1021/acsami.8b06764
ACS Appl. Mater. Interfaces 2018, 10, 20368−20376

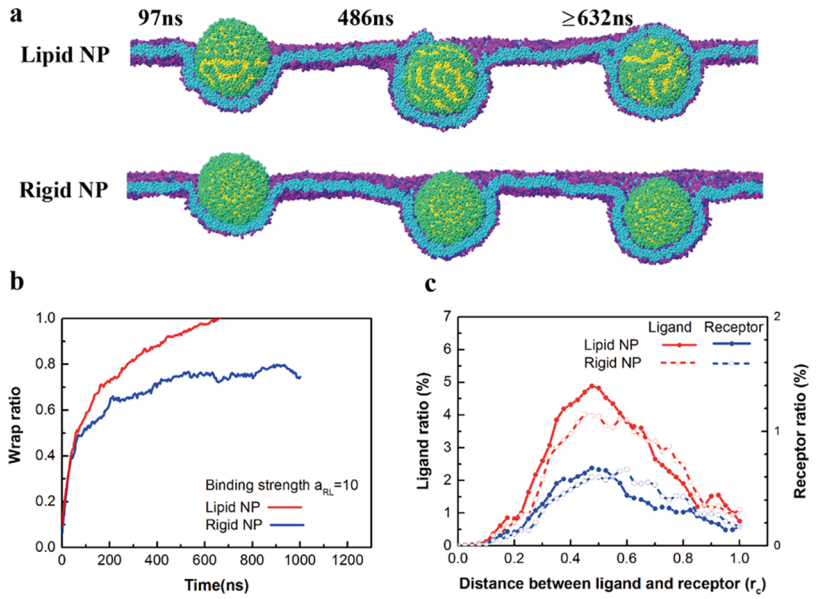


**Figure 3.** Effect of the deformation of the lipid shell on the endocytosis of NP at a low ligand−receptor binding strength ($a_{RL}$ = 10). (a) Typical snapshots for the endocytosis of the lipid NP and the rigid NP. (b) Time evolution of the wrapping ratio. (c) Ratio of binding ligands or receptors to total ligands or receptors at a different distance at the contact region. Neighboring values are selected within a distance of about 0.025$r_c$.

change in coating flexible molecules is one of the influences on the interaction between NPs and biomembranes.[5,40] Therefore, the energy consumed for such deformation of the coatings should be taken into account for analyzing the endocytosis kinetics of the lipid NPs.

Besides the energy cost for the deformation of the coating surfactant lipids, other two main factors influence the endocytosis of the lipid NPs. The first one is the bending energy of the cell membrane, which is $F_{bending} = 8\pi B$ for a fully wrapped NP, where $B$ is the bending rigidity for the membrane.[9] Note that the bending energy is a constant independent of the physicochemical properties of NP. The second one is the adhesion energy between the NP and the membrane, driven by specific and nonspecific interactions.[61] The specific interaction is provided by the ligand−receptor interaction that is controlled by the binding number and binding strength of the ligands and the receptors,[62,63] while the nonspecific interaction mainly stems from the hydrophobicity of the lipid NP. The number of the coating ligands and the hydrophobicity of the lipid NP depend on the coating density of the surfactant lipids. The binding strength of the ligands and the receptors denotes the different cellular responses to the lipid NP. As discussed above, to acquire a total engulfment of the lipid NP, the adhesion energy must overcome the energy cost consisted by membrane bending and deformation of the coating lipids. In consideration of the bending energy only depending on the rigidity of the cell membrane, we mainly investigate how the deformation of the coating lipids and the density of the coating lipids affect the endocytosis of lipid NPs at different binding strengths of the ligands and receptors.

### 3.2. Effect of the Deformation of the Coating Lipids.

We assume a rigid NP that has the same surface properties as the lipid NP but is unable to deform. Our simulations show that these two NPs suffer the different fates when encountering the same membrane (Figures 3a and 4a). At a low receptor−ligand binding strength ($a_{RL}$ = 10), the lipid NP can be totally engulfed by the membrane, whereas the rigid NP cannot (Figure 3a,b). Figure 3a shows that a monolayer protrusion can promote the total engulfment of the lipid NP but is absent in the endocytosis of the rigid NP. To explain this phenomenon, we examine the ligand−receptor distributions at the binding range ($r_c \leq 1$) in the contact region for both the NPs. Here, the ratio of binding ligands or receptors to total ligands or receptors denotes their distributions within the binding range (Figure 3c). We notice that the lipid NP has more ligands involved in reacting with the membrane receptors than the rigid NP without consuming extra receptors. Besides, the ligands on the lipid NP can bind with the receptors more closely than those on the rigid NP, resulting in a higher binding energy. These results demonstrate that the flexible lipids can adjust their posture for a better binding condition with receptors and hence provide more adhesion energy to promote the total engulfment. Recently, Xia et al. found that longer coating ligands on the NPs will be rearranged during the endocytosis to help the total engulfment of NPs, whereas the shorter ones cannot.[64] They demonstrated that the mobile ability of the coatings can promote the endocytosis, which confirms our finding that the deformation of the coating lipids from the homogeneous ones to the patterned ones can be beneficial for the endocytosis.

However, when the ligand−receptor binding strength increases to $a_{RL}$ = 0, the rigid NP undergoes faster engulfment by the cell membrane than the lipid NP (Figure 4a), as the energy loss for the deformation of the coating lipids increases with the binding strength and thus delays the endocytosis. The deformation of the lipid NP can be divided into two parts: the stretching or compression of the soft shell at the radial direction, which is considered as one important role in cellular uptake,[39,65] and the conformational changes of the head groups as shown previously in Figure 3a. From Figure 4b, we find that there is almost no difference in the density distribution of the surfactant lipid beads between the lipid NP and the rigid NP. Therefore, the lipid NP does not deform at the radial direction because of the high elasticity modulus and small thickness of the lipid shell. Besides, for the lipid NP, there exists a left peak shift of the membrane lipid beads (MLBs), as the MLB can


DOI: 10.1021/acsami.8b06764
ACS Appl. Mater. Interfaces 2018, 10, 20368−20376

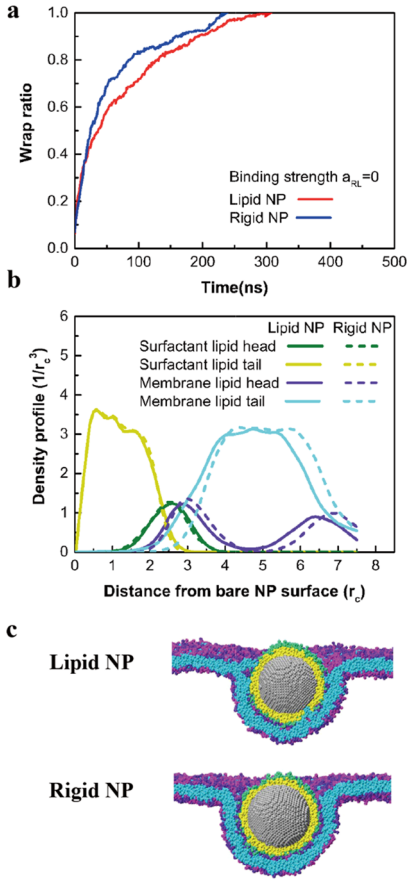


**Figure 4.** Effect of the deformation of the lipid shell on the endocytosis of NP at a high ligand−receptor binding strength ($a_{RL}$ = 0). (a) Time evolution of the wrapping ratio of the lipid NP and rigid NP. (b) Density profile of different beads at a different distance away from the core NP. The colors of the curves for different beads are consistent with the colors shown in snapshots. (c) Detailed illustration for the deformation of the lipid shell compared with a rigid shell. The membrane and shell are shown in the cross-sectional view particularly.

enter into the lipid shell after the redistributions of the head groups of the coating lipids (Figure 4b,c). These results prove that obvious conformational changes occur at the interface between the lipid NP and the membrane. The energy loss for such deformation will eventually delay the endocytosis at a high binding strength, even though the deformation can provide more adhesion energy. Collectively, we conclude that the deformation of the coating lipid shell controls both the energy consumed for the deformation and adhesion energy with the membrane, thus affecting the cellular uptake. In practice, nanocarriers, such as mesoporous silica NP and RNA,[66,67] are usually incubated in the lipid matrix binding types of lipids to promote its biocompatibility. It would be beneficial for cellular uptake to determine an optimal rigidity of the binding lipids by altering the incubation temperature and the lipid components.

**3.3. Effect of the Coating Lipid Density.** The coating lipid density of the NP often varies with the incubation environment in pulmonary surfactant solutions and the physicochemical properties of the pristine NP, such as surface modification and curvature.[27,68] In our simulations, three different coating lipid numbers are set to be 600, 800, and 1000, with an increase in ligand density and a decrease in hydrophobicity. The hydrophobicities of each NP are 0.48, 0.37, and 0.29 calculated from the equilibrated lipid NPs, where the hydrophobicity is characterized by the proportion of the hydrophobic solvent-accessible surface beads to the total solvent-accessible surface beads. These NPs undergo different endocytosis kinetics under varieties of ligand−receptor binding strength ($a_{RL}$: 13−0, $\varepsilon$: 3−5). The simulation results are summarized into a phase diagram, as shown in Figure 5a. When

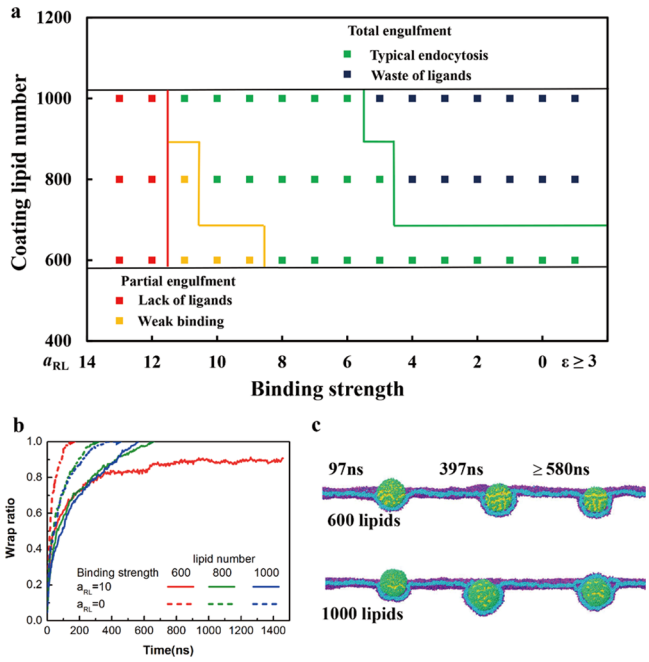


**Figure 5.** Roles of the density of the coating lipid density in the endocytosis of NP at different binding strengths. (a) Phase diagram for the endocytosis of the lipid NPs, and it is given as a function of the ligand−receptor binding strength and coating lipid number. (b) Time evolution of the wrapping ratio at different binding strengths. (c) Typical snapshots for the endocytosis of the lipid NPs with different coating lipid numbers at a low binding strength ($a_{RL}$ = 10).

the binding strength is low, none of the NPs can be engulfed by the membrane because of their weak binding ability with the receptors, which is called the weak binding region. As the binding strength increases to $a_{RL}$ = 10, the NP coated with 600 lipids can only be partially wrapped by the membrane, while other NPs are totally wrapped by the membrane (Figure 5b,c). However, at the initial stage of endocytosis, the 600-lipid-coated NP can be wrapped faster than other NPs because of its higher hydrophobicity. This implies that the nonspecific interaction can spontaneously affect the endocytosis once the NPs adhere to the membrane, whereas the specific interaction needs a time delay in accordance with current theoretic models.[9,10] As time goes, all of these NPs move downward and are gradually wrapped by the membrane. At a certain moment, the 600-lipid-coated NP cannot be wrapped anymore. However, for other NPs, taking the 1000-lipid-coated NP, for example, there is a monolayer protrusion promoting the total engulfment of the NPs (Figure 5c). The failure of the monolayer protrusion results from the lack of the ligands at the noncontact region and the weak binding interaction at the contact region. With the increase of the binding strength, all of the NPs can be totally engulfed by the membrane. Beyond this point, coating more lipids is not beneficial anymore and instead leads to a longer wrapping time, leading to the waste of the ligands. Take a high binding strength ($a_{RL}$ = 0), for example,


DOI: 10.1021/acsami.8b06764
ACS Appl. Mater. Interfaces 2018, 10, 20368−20376

the 600-lipid-coated NP takes the shortest time for the total endocytosis as shown in Figure 5b. Generally, the binding strength between the NPs and the membrane is a key factor in evaluating the cellular uptake of lipid NPs.

To further study the role of the coating lipid density in cellular uptake, we check the ligand−receptor distributions at the contact region for the 600-lipid-coated NP and the 1000-lipid-coated NP (Figure 6a). For the 1000-lipid-coated NP, more ligands interact with receptors to provide more adhesion energy. Surprisingly, the in-pair ligand ratio for the 1000-lipid-coated NP is even higher than for the 600-lipid-coated NP. Such high lipid density can not only provide with more ligands for specific interactions but also promote the continuous and uniform distributions of the ligands, resulting in an enhanced binding efficiency at a low binding strength. Furthermore, the NPs coated with more lipids consume more receptors to accomplish the endocytosis (Figure 6a). We also examine the initial distribution of these receptors, where the receptors required for the total engulfment of the 1000-lipid-coated NP are more broadly distributed in the membrane than that for the 600-lipid-coated NP (Figure 6c). It shows that for the 1000-lipid-coated NP, more receptors have to undergo a longer diffusion process to reach on the NP surface, leading to a longer time of the full engulfment. Meanwhile, by comparing the head group distributions between these NPs, the coating density only influences the density of binding receptors (see Figure 6a,c), without altering the total density of binding membrane lipids and receptors (Figure 6b). This means that for a higher lipid-coated NP, some receptors may replace the membrane lipids at the interface between the NP and the membrane, thus delaying the total endocytosis. Moreover, from the entry perspective of multi-NPs, the number of the receptors in the cell membrane is limited. Optimal ligand density may vary with the binding strength and coating extra ligands can result in a receptor-shortage phenomenon and weaker cellular uptake.[62] Recent experimental results have demonstrated that the cellular uptake of NPs decreased at a high surfactant lipid coverage, which was in line with our analysis.[68] Our simulations demonstrate that exposed hydrophobic tails of the coating lipids can also affect the endocytosis process of the lipid NP. Figure 6b illustrates that there are some membrane lipid tails close to the NP surface for the 600-lipid-coated NP, proving that the lipids of the cell membrane can enter into the interior of the coating lipids. The detailed snapshots in Figure 6d clearly show that the membrane lipids can diffuse to the NP surface before the membrane wraps the NP. For the 600-lipid-NP, the unsaturation of the lipid coating leads to few hydrophobic tails of the coating lipids exposed in water, causing an increase in hydrophobicity. As a result, the membrane lipids can be extracted to the hydrophobic solvent-accessible surface, which is similar in the observation of the graphene−cell membrane interaction.[69] Both the hydrophilic and hydrophobic fractions of the coating lipids affect the endocytosis process of lipid NPs, although the hydrophilic one relies on the specific interactions with the receptors on the membrane, whereas the hydrophobic one enhances the nonspecific interaction between the NP and the membrane.

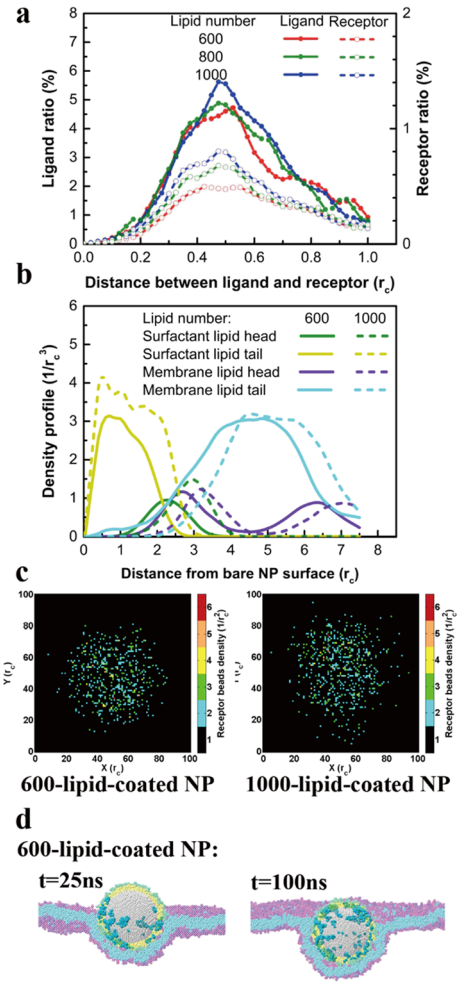


**Figure 6.** Effect of the lipid density on some main factors in cellular uptake. (a) Ratio of binding ligands or receptors to total ligands or receptors at a different distance for lipid NPs at a low binding strength ($a_{RL}$ = 10). (b) Density profile of different beads at a different distance away from the core NP for totally engulfed lipid NPs. (c) Illustration of the initial density distribution of the receptors consumed for the total engulfment of the 600-lipid-coated NP and 1000-lipid-coated NP. (d) Representative snapshots for the lipid extraction by the unsaturated (600-lipid-coated) NP. Cyan beads represent membrane lipid tails that are within about 1.0$r_c$ around the NP surface, and other beads are transparent for clarity.

**3.4. Effect of the Coating Hydrophobic SP.** To study the effect of hydrophobic SPs on the endocytosis, we compare the endocytosis process of the lipoprotein NPs and lipid NPs. The molar ratio of the SPs on the coatings is set to 0.01, consistent to our previous simulation work.[28] When the lipoprotein NPs interact with the membrane at a low ligand−receptor binding strength, the SPs will first contact with the cell membrane through the rotation of the NPs because of their hydrophobicity and strong attraction to the membrane lipids (Figure 7a). In addition, by comparing the endocytosis dynamics of the lipid NPs and lipoprotein NPs, we notice that hydrophobic SPs can accelerate the endocytosis and promote the membrane wrapping the lipoprotein NPs, especially as they come in contact with the membrane (see Figure 7a,b). However, for lipoprotein NPs, the lack of the ligands at the noncontact region will lead to a frustrated endocytosis at a lower ligand−receptor binding strength (Figure 7a), even though the coating proteins can increase the adhesion energy. At a higher binding strength, coating with extra hydrophobic SPs (800-lipid-coated NP and 1000-lipid-coated NP), unlike the ligands as surfactant lipids, can increase the wrapping speed as shown in Figure 7c. This is because the coating SPs can increase the adhesion energy by binding tightly


DOI: 10.1021/acsami.8b06764
ACS Appl. Mater. Interfaces 2018, 10, 20368−20376

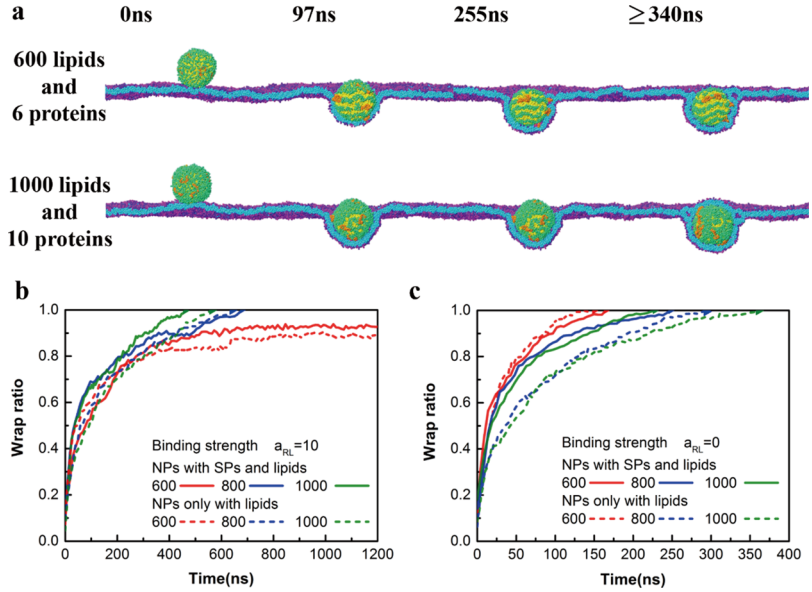


**Figure 7.** Effect of the coating hydrophobic SPs on the endocytosis of the NPs. (a) Typical snapshots for the endocytosis of the lipoprotein NPs with different coating densities at a low ligand−receptor binding strength ($a_{RL}$ = 10). (b) Time evolution of the wrapping ratio for lipoprotein NPs with different coating densities at a low ligand−receptor binding strength ($a_{RL}$ = 10) compared with the lipid NPs. (c) Time evolution of the wrapping ratio for lipoprotein NPs with different coating densities at a high ligand−receptor binding strength ($a_{RL}$ = 0) compared with the lipid NPs.

with the membrane lipids without intensifying the receptor diffusion and competition.[45,46] At some circumstances (the 800-lipid-coated NP at $a_{RL}$ = 10 and the 600-lipid-coated NP at $a_{RL}$ = 0), coating with extra SPs can also slightly influence the distribution of the coating lipids on NPs. The endocytosis of the lipoprotein NPs is somehow delayed at the end of the endocytosis, resulted from the decrease of the ligands at the noncontact region. Previous in vitro experiments found that the uptake of NPs coated with the pulmonary surfactant by macrophages mainly depends on the lipid coating and is only slightly affected by the hydrophilic SPs.[49,70] Our simulation results show that the engulfment efficiency mainly depends on the lipid density because of their overwhelming coverage ratio. It is more beneficial for the uptake of the lipid NPs by additionally coating with biomolecules (e.g., hydrophobic SPs) that can anchor on the membrane rather than coating extra molecules with the same ligands (surfactant lipids).

Although the CG simulation can help understand the endocytosis mechanism of the NPs at the mesoscale, there still exist several limitations in this research. First, compared with the real bioenvironment, both the temporal and spatial scales of the simulation are much smaller. Second, because of intrinsic "smearing" of the atomic details in the CG methodology, the present simulation is unable to consider more detailed features of the NP−membrane interaction, such as the hydration force, the structural and functional changes of the biomacromolecules, and the interaction of each functional group within the molecules, which may be important in examining the nanotoxicology of the NPs.[5] Third, the natural pulmonary surfactant is much more complicated. The charge and the type of the lipid heads, the length of the lipid tails, and the type of the SP probably affect the endocytosis of the NPs coated with surfactant lipids, which is worthy of future investigation.

## 4. CONCLUSIONS

Through a DPD simulation study, we find that the pulmonary surfactant corona can provide the biorecognition to promote the RME for NPs. More importantly, we study the effect of the properties of surfactant lipids and hydrophobic SPs on the endocytosis of NPs. First, our results show that the lipid NP can bind with more receptors because of the flexibility of the coating lipids when compared with an assumed rigid NP, which can promote the total engulfment of the lipid NP at a low ligand−receptor binding strength. However, with the increase of the ligand−receptor binding strength, the energy cost for the deformations of the coating lipids will finally delay the endocytosis although this deformation can provide more adhesion energy. Second, our results demonstrate that the coating lipid density also plays a crucial role in the RME. For the unsaturated coated lipid NP, the hydrophobicity provided by the exposed surfactant lipid tails can accelerate the wrapping process once the NP attaches to the membrane. However, the lack of the ligands will lead to a partial engulfment owing to the failure of the monolayer membrane protrusion. In addition, the ligand−receptor binding strength also has an important role in the endocytosis efficiency. At a high binding strength, coating with more lipids will intensify the competition for receptors around the NP surface, leading to a longer endocytosis time. Moreover, from a viewpoint of multiple NPs' endocytosis, the receptors consumed for the endocytosis are limited. Thus, the optimal ligand density varied with the binding strength should be taken seriously for the endocytosis of corona-NPs and designing NPs for drug delivery. Finally, we study the effect of hydrophobic SPs on the endocytosis of NPs, by comparing the endocytosis process of the lipoprotein NPs and lipid NPs. We find that the hydrophobic SPs can promote the uptake of NPs owing to their extra attraction to the membrane lipids. However, the engulfment efficiency mainly relies on the density of the coating lipids because of their overwhelming coverage ratio. Generally, our mesoscale computational results can help understand the RME mechanics for NPs coated with


DOI: 10.1021/acsami.8b06764
ACS Appl. Mater. Interfaces 2018, 10, 20368−20376

the pulmonary surfactant from a molecular view and provide some useful guidelines for designing inhaled NPs for drug delivery to lungs.

## ■ ASSOCIATED CONTENT

### Supporting Information

The Supporting Information is available free of charge on the ACS Publications website at DOI: 10.1021/acsami.8b06764.

Detailed parameterization for the CG models; sample for the LAMMPS input script; and script to create the bond list for the DPD protein (PDF)

## ■ AUTHOR INFORMATION


### Corresponding Authors

*E-mail: guoqing.hu@imech.ac.cn (G.H.).
*E-mail: sjliu@rcees.ac.cn (S.L.).

### ORCID

Xuan Bai: 0000-0001-5593-9427
Ming Xu: 0000-0002-4499-6116
Sijin Liu: 0000-0002-5643-0734
Guoqing Hu: 0000-0001-9451-5336


### Notes

The authors declare no competing financial interest.

## ■ ACKNOWLEDGMENTS

This work was supported by NSFC (91543125, 11572334, 21425731, and 21637004), the CAS Key Research Program of Frontier Sciences (QYZDB-SSW-JSC036), the CAS Strategic Priority Research Program (XDB22040403 and XDB14000000), and a national "973" program (grant no. 2014CB932000). The MD simulations were performed on TianHe-1(A) at the National Supercomputing Center in Tianjin.

## ■ REFERENCES


(1) Petros, R. A.; DeSimone, J. M. Strategies in the Design of Nanoparticles for Therapeutic Applications. *Nat. Rev. Drug Discovery* **2010**, *9*, 615−627.
(2) Sharma, P.; Brown, S.; Walter, G.; Santra, S.; Moudgil, B. Nanoparticles for Bioimaging. *Adv. Colloid Interface Sci.* **2006**, *123*−*126*, 471−485.
(3) Nel, A.; Xia, T.; Mädler, L.; Li, N. Toxic Potential of Materials at the Nanolevel. *Science* **2006**, *311*, 622−627.
(4) Oberdörster, G.; Oberdörster, E.; Oberdörster, J. Nanotoxicology: An Emerging Discipline Evolving from Studies of Ultrafine Particles. *Environ. Health Perspect.* **2005**, *113*, 823−839.
(5) Nel, A. E.; Mädler, L.; Velegol, D.; Xia, T.; Hoek, E. M. V.; Somasundaran, P.; Klaessig, F.; Castranova, V.; Thompson, M. Understanding Biophysicochemical Interactions at the Nano-Bio Interface. *Nat. Mater.* **2009**, *8*, 543−557.
(6) Elsaesser, A.; Howard, C. V. Toxicology of Nanoparticles. *Adv. Drug Delivery Rev.* **2012**, *64*, 129−137.
(7) Sahay, G.; Alakhova, D. Y.; Kabanov, A. V. Endocytosis of Nanomedicines. *J. Controlled Release* **2010**, *145*, 182−195.
(8) Chou, L. Y. T.; Ming, K.; Chan, W. C. W. Strategies for the Intracellular Delivery of Nanoparticles. *Chem. Soc. Rev.* **2011**, *40*, 233−245.
(9) Zhang, S.; Gao, H.; Bao, G. Physical Principles of Nanoparticle Cellular Endocytosis. *ACS Nano* **2015**, *9*, 8655−8671.
(10) Gao, H.; Shi, W.; Freund, L. B. Mechanics of Receptor-Mediated Endocytosis. *Proc. Natl. Acad. Sci. U.S.A.* **2005**, *102*, 9469−9474.
(11) Zhang, S.; Li, J.; Lykotrafitis, G.; Bao, G.; Suresh, S. Size-Dependent Endocytosis of Nanoparticles. *Adv. Mater.* **2009**, *21*, 419−424.
(12) Chithrani, B. D.; Ghazani, A. A.; Chan, W. C. W. Determining the Size and Shape Dependence of Gold Nanoparticle Uptake into Mammalian Cells. *Nano Lett.* **2006**, *6*, 662−668.
(13) Gratton, S. E. A.; Ropp, P. A.; Pohlhaus, P. D.; Luft, J. C.; Madden, V. J.; Napier, M. E.; DeSimone, J. M. The Effect of Particle Design on Cellular Internalization Pathways. *Proc. Natl. Acad. Sci. U.S.A.* **2008**, *105*, 11613−11618.
(14) Li, Y.; Zhang, X.; Cao, D. Nanoparticle Hardness Controls the Internalization Pathway for Drug Delivery. *Nanoscale* **2015**, *7*, 2758−2769.
(15) Yi, X.; Shi, X.; Gao, H. Cellular Uptake of Elastic Nanoparticles. *Phys. Rev. Lett.* **2011**, *107*, 098101.
(16) Ding, H.-m.; Ma, Y.-q. Theoretical and Computational Investigations of Nanoparticle-Biomembrane Interactions in Cellular Delivery. *Small* **2015**, *11*, 1055−1071.
(17) Docter, D.; Westmeier, D.; Markiewicz, M.; Stolte, S.; Knauer, S. K.; Stauber, R. H. The Nanoparticle Biomolecule Corona: Lessons Learned—Challenge Accepted? *Chem. Soc. Rev.* **2015**, *44*, 6094−6121.
(18) Walkey, C. D.; Chan, W. C. W. Understanding and Controlling the Interaction of Nanomaterials with Proteins in a Physiological Environment. *Chem. Soc. Rev.* **2012**, *41*, 2780−2799.
(19) Monopoli, M. P.; Åberg, C.; Salvati, A.; Dawson, K. A. Biomolecular Coronas Provide the Biological Identity of Nanosized Materials. *Nat. Nanotechnol.* **2012**, *7*, 779−786.
(20) Lesniak, A.; Fenaroli, F.; Monopoli, M. R.; Åberg, C.; Dawson, K. A.; Salvati, A. Effects of the Presence or Absence of a Protein Corona on Silica Nanoparticle Uptake and Impact on Cells. *ACS Nano* **2012**, *6*, 5845−5857.
(21) Salvati, A.; Pitek, A. S.; Monopoli, M. P.; Prapainop, K.; Bombelli, F. B.; Hristov, D. R.; Kelly, P. M.; Åberg, C.; Mahon, E.; Dawson, K. A. Transferrin-Functionalized Nanoparticles Lose Their Targeting Capabilities When a Biomolecule Corona Adsorbs on the Surface. *Nat. Nanotechnol.* **2013**, *8*, 137−143.
(22) Ritz, S.; Schöttler, S.; Kotman, N.; Baier, G.; Musyanovych, A.; Kuharev, J.; Landfester, K.; Schild, H.; Jahn, O.; Tenzer, S.; Mailänder, V. Protein Corona of Nanoparticles: Distinct Proteins Regulate the Cellular Uptake. *Biomacromolecules* **2015**, *16*, 1311−1321.
(23) Tedja, R.; Lim, M.; Amal, R.; Marquis, C. Effects of Serum Adsorption on Cellular Uptake Profile and Consequent Impact of Titanium Dioxide Nanoparticles on Human Lung Cell Lines. *ACS Nano* **2012**, *6*, 4083−4093.
(24) Hu, G.; Jiao, B.; Shi, X.; Valle, R. P.; Fan, Q.; Zuo, Y. Y. Physicochemical Properties of Nanoparticles Regulate Translocation across Pulmonary Surfactant Monolayer and Formation of Lipoprotein Corona. *ACS Nano* **2013**, *7*, 10525−10533.
(25) Sung, J. C.; Pulliam, B. L.; Edwards, D. A. Nanoparticles for Drug Delivery to the Lungs. *Trends Biotechnol.* **2007**, *25*, 563−570.
(26) Gasser, M.; Rothen-Rutishauser, B.; Krug, H. F.; Gehr, P.; Nelle, M.; Yan, B.; Wick, P. The Adsorption of Biomolecules to Multi-Walled Carbon Nanotubes Is Influenced by Both Pulmonary Surfactant Lipids and Surface Chemistry. *J. Nanobiotechnol.* **2010**, *8*, 31.
(27) Raesch, S. S.; Tenzer, S.; Storck, W.; Rurainski, A.; Selzer, D.; Ruge, C. A.; Perez-Gil, J.; Schaefer, U. F.; Lehr, C.-M. Proteomic and Lipidomic Analysis of Nanoparticle Corona Upon Contact with Lung Surfactant Reveals Differences in Protein, but Not Lipid Composition. *ACS Nano* **2015**, *9*, 11872−11885.
(28) Hu, Q.; Bai, X.; Hu, G.; Zuo, Y. Y. Unveiling the Molecular Structure of Pulmonary Surfactant Corona on Nanoparticles. *ACS Nano* **2017**, *11*, 6832−6842.
(29) Thorley, A. J.; Ruenraroengsak, P.; Potter, T. E.; Tetley, T. D. Critical Determinants of Uptake and Translocation of Nanoparticles by the Human Pulmonary Alveolar Epithelium. *ACS Nano* **2014**, *8*, 11778−11789.
(30) Theodorou, I. G.; Ruenraroengsak, P.; Gow, A.; Schwander, S.; Zhang, J.; Chung, K. F.; Tetley, T. D.; Ryan, M. P.; Porter, A. E. Effect of Pulmonary Surfactant on the Dissolution, Stability and Uptake of




DOI: 10.1021/acsami.8b06764
ACS Appl. Mater. Interfaces 2018, 10, 20368−20376

Zinc Oxide Nanowires by Human Respiratory Epithelial Cells. *Nanotoxicology* **2016**, *10*, 1351−1362.
(31) Gasser, M.; Wick, P.; Clift, M. J. D.; Blank, F.; Diener, L.; Yan, B.; Gehr, P.; Krug, H. F.; Rothen-Rutishauser, B. Pulmonary Surfactant Coating of Multi-Walled Carbon Nanotubes (MWCNTs) Influences Their Oxidative and Pro-Inflammatory Potential in Vitro. *Part. Fibre Toxicol.* **2012**, *9*, 17.
(32) Martins, S.; Costa-Lima, S.; Carneiro, T.; Cordeiro-da-Silva, A.; Souto, E. B.; Ferreira, D. C. Solid Lipid Nanoparticles as Intracellular Drug Transporters: An Investigation of the Uptake Mechanism and Pathway. *Int. J. Pharm.* **2012**, *430*, 216−227.
(33) Shi, X.; von dem Bussche, A.; Hurt, R. H.; Kane, A. B.; Gao, H. Cell Entry of One-Dimensional Nanomaterials Occurs by Tip Recognition and Rotation. *Nat. Nanotechnol.* **2011**, *6*, 714−719.
(34) Yang, K.; Ma, Y.-Q. Computer Simulation of the Translocation of Nanoparticles with Different Shapes across a Lipid Bilayer. *Nat. Nanotechnol.* **2010**, *5*, 579−583.
(35) Vácha, R.; Martinez-Veracoechea, F. J.; Frenkel, D. Receptor-Mediated Endocytosis of Nanoparticles of Various Shapes. *Nano Lett.* **2011**, *11*, 5391−5395.
(36) Yue, T.; Zhang, X. Molecular Understanding of Receptor-Mediated Membrane Responses to Ligand-Coated Nanoparticles. *Soft Matter* **2011**, *7*, 9104−9112.
(37) Smith, K. A.; Jasnow, D.; Balazs, A. C. Designing Synthetic Vesicles That Engulf Nanoscopic Particles. *J. Chem. Phys.* **2007**, *127*, 084703.
(38) Nangia, S.; Sureshkumar, R. Effects of Nanoparticle Charge and Shape Anisotropy on Translocation through Cell Membranes. *Langmuir* **2012**, *28*, 17666−17671.
(39) Ding, H.-m.; Ma, Y.-q. Role of Physicochemical Properties of Coating Ligands in Receptor-Mediated Endocytosis of Nanoparticles. *Biomaterials* **2012**, *33*, 5798−5802.
(40) Li, Y.; Kröger, M.; Liu, W. K. Endocytosis of Pegylated Nanoparticles Accompanied by Structural and Free Energy Changes of the Grafted Polyethylene Glycol. *Biomaterials* **2014**, *35*, 8467−8478.
(41) Ding, H.-m.; Ma, Y.-q. Computer Simulation of the Role of Protein Corona in Cellular Delivery of Nanoparticles. *Biomaterials* **2014**, *35*, 8703−8710.
(42) Groot, R. D.; Warren, P. B. Dissipative Particle Dynamics: Bridging the Gap between Atomistic and Mesoscopic Simulation. *J. Chem. Phys.* **1997**, *107*, 4423−4435.
(43) Ramazani, A.; Mandal, T.; Larson, R. G. Modeling the Hydrophobicity of Nanoparticles and Their Interaction with Lipids and Proteins. *Langmuir* **2016**, *32*, 13084−13094.
(44) Mandal, B.; Bhattacharjee, H.; Mittal, N.; Sah, H.; Balabathula, P.; Thoma, L. A.; Wood, G. C. Core-Shell-Type Lipid-Polymer Hybrid Nanoparticles as a Drug Delivery Platform. *Nanomedicine* **2013**, *9*, 474−491.
(45) Whitsett, J. A.; Weaver, T. E. Hydrophobic Surfactant Proteins in Lung Function and Disease. *N. Engl. J. Med.* **2002**, *347*, 2141−2148.
(46) Serrano, A. G.; Pérez-Gil, J. Protein-Lipid Interactions and Surface Activity in the Pulmonary Surfactant System. *Chem. Phys. Lipids* **2006**, *141*, 105−118.
(47) Groot, R. D.; Rabone, K. L. Mesoscopic Simulation of Cell Membrane Damage, Morphology Change and Rupture by Nonionic Surfactants. *Biophys. J.* **2001**, *81*, 725−736.
(48) Plimpton, S. Fast Parallel Algorithms for Short-Range Molecular Dynamics. *J. Comput. Phys.* **1995**, *117*, 1−19.
(49) Kapralov, A. A.; Feng, W. H.; Amoscato, A. A.; Yanamala, N.; Balasubramanian, K.; Winnica, D. E.; Kisin, E. R.; Kotchey, G. P.; Gou, P.; Sparvero, L. J.; Ray, P.; Mallampalli, R. K.; Klein-Seetharaman, J.; Fadeel, B.; Star, A.; Shvedova, A. A.; Kagan, V. E. Adsorption of Surfactant Lipids by Single-Walled Carbon Nanotubes in Mouse Lung Upon Pharyngeal Aspiration. *ACS Nano* **2012**, *6*, 4147−4156.
(50) Yue, T.; Zhang, X. Molecular Modeling of the Pathways of Vesicle−Membrane Interaction. *Soft Matter* **2013**, *9*, 559−569.
(51) Zorko, M.; Langel, U. Cell-Penetrating Peptides: Mechanism and Kinetics of Cargo Delivery. *Adv. Drug Delivery Rev.* **2005**, *57*, 529−545.
(52) Shillcock, J. C.; Lipowsky, R. Tension-Induced Fusion of Bilayer Membranes and Vesicles. *Nat. Mater.* **2005**, *4*, 225−228.
(53) Li, X.; Liu, Y.; Wang, L.; Deng, M.; Liang, H. Fusion and Fission Pathways of Vesicles from Amphiphilic Triblock Copolymers: A Dissipative Particle Dynamics Simulation Study. *Phys. Chem. Chem. Phys.* **2009**, *11*, 4051−4059.
(54) Li, Y.; Li, X.; Li, Z.; Gao, H. Surface-Structure-Regulated Penetration of Nanoparticles across a Cell Membrane. *Nanoscale* **2012**, *4*, 3768−3775.
(55) Ding, H.-m.; Tian, W.-d.; Ma, Y.-q. Designing Nanoparticle Translocation through Membranes by Computer Simulations. *ACS Nano* **2012**, *6*, 1230−1238.
(56) Bothun, G. D. Hydrophobic Silver Nanoparticles Trapped in Lipid Bilayers: Size Distribution, Bilayer Phase Behavior, and Optical Properties. *J. Nanobiotechnol.* **2008**, *6*, 13.
(57) Yue, T.; Zhang, X.; Huang, F. Membrane Monolayer Protrusion Mediates a New Nanoparticle Wrapping Pathway. *Soft Matter* **2014**, *10*, 2024−2034.
(58) Footer, M. J.; Kerssemakers, J. W. J.; Theriot, J. A.; Dogterom, M. Direct Measurement of Force Generation by Actin Filament Polymerization Using an Optical Trap. *Proc. Natl. Acad. Sci. U.S.A.* **2007**, *104*, 2181−2186.
(59) Mousseau, F.; Puisney, C.; Mornet, S.; Borgne, R. L.; Vacher, A.; Airiau, M.; Baeza-Squiban, A.; Berret, J.-F. Supported Pulmonary Surfactant Bilayers on Silica Nanoparticles: Formulation, Stability and Impact on Lung Epithelial Cells. *Nanoscale* **2017**, *9*, 14967−14978.
(60) Stevens, M. J.; Hoh, J. H.; Woolf, T. B. Insights into the Molecular Mechanism of Membrane Fusion from Simulation: Evidence for the Association of Splayed Tails. *Phys. Rev. Lett.* **2003**, *91*, 188102.
(61) Decuzzi, P.; Ferrari, M. The Role of Specific and Non-Specific Interactions in Receptor-Mediated Endocytosis of Nanoparticles. *Biomaterials* **2007**, *28*, 2915−2922.
(62) Yuan, H.; Li, J.; Bao, G.; Zhang, S. Variable Nanoparticle-Cell Adhesion Strength Regulates Cellular Uptake. *Phys. Rev. Lett.* **2010**, *105*, 138101.
(63) Yuan, H.; Zhang, S. Effects of Particle Size and Ligand Density on the Kinetics of Receptor-Mediated Endocytosis of Nanoparticles. *Appl. Phys. Lett.* **2010**, *96*, 033704.
(64) Xia, Q.-s.; Ding, H.-m.; Ma, Y.-q. Can Dual-Ligand Targeting Enhance Cellular Uptake of Nanoparticles? *Nanoscale* **2017**, *9*, 8982−8989.
(65) Sun, J.; Zhang, L.; Wang, J.; Feng, Q.; Liu, D.; Yin, Q.; Xu, D.; Wei, Y.; Ding, B.; Shi, X.; Jiang, X. Tunable Rigidity of (Polymeric Core)-(Lipid Shell) Nanoparticles for Regulated Cellular Uptake. *Adv. Mater.* **2015**, *27*, 1402−1407.
(66) Yang, Y.; Song, W.; Wang, A.; Zhu, P.; Fei, J.; Li, J. Lipid Coated Mesoporous Silica Nanoparticles as Photosensitive Drug Carriers. *Phys. Chem. Chem. Phys.* **2010**, *12*, 4418−4422.
(67) Hidalgo, A.; Cruz, A.; Pérez-Gil, J. Pulmonary Surfactant and Nanocarriers: Toxicity Versus Combined Nanomedical Applications. *Biochim. Biophys. Acta* **2017**, *1859*, 1740−1748.
(68) Wohlleben, W.; Driessen, M. D.; Raesch, S.; Schaefer, U. F.; Schulze, C.; von Vacano, B.; Vennemann, A.; Wiemann, M.; Ruge, C. A.; Platsch, H.; Mues, S.; Ossig, R.; Tomm, J. M.; Schnekenburger, J.; Kuhlbusch, T. A. J.; Luch, A.; Lehr, C.-M.; Haase, A. Influence of Agglomeration and Specific Lung Lining Lipid/Protein Interaction on Short-Term Inhalation Toxicity. *Nanotoxicology* **2016**, *10*, 970−980.
(69) Tu, Y.; Lv, M.; Xiu, P.; Huynh, T.; Zhang, M.; Castelli, M.; Liu, Z.; Huang, Q.; Fan, C.; Fang, H.; Zhou, R. Destructive Extraction of Phospholipids from Escherichia Coli Membranes by Graphene Nanosheets. *Nat. Nanotechnol.* **2013**, *8*, 594−601.
(70) Ruge, C. A.; Schaefer, U. F.; Herrmann, J.; Kirch, J.; Cañadas, O.; Echaide, M.; Pérez-Gil, J.; Casals, C.; Müller, R.; Lehr, C.-M. The Interplay of Lung Surfactant Proteins and Lipids Assimilates the Macrophage Clearance of Nanoparticles. *PLoS One* **2012**, *7*, e40775.


DOI: 10.1021/acsami.8b06764
*ACS Appl. Mater. Interfaces* 2018, 10, 20368−20376